BIOCHEMISTRY
including biophysical chemistry & molecular biology

Article

pubs.acs.org/biochemistry

Crystal Structures of Polymorphic Prion Protein β1 Peptides Reveal Variable Steric Zipper Conformations

Lu Yu, Seung-Joo Lee,† and Vivien C. Yee*

Department of Biochemistry, Case Western Reserve University, Cleveland, Ohio 44106, United States

Supporting Information

ABSTRACT: The pathogenesis of prion diseases is associated with the conformational conversion of normal, predominantly α-helical prion protein (PrP^C) into a pathogenic form that is enriched with β-sheets (PrP^{Sc}). Several PrP^C crystal structures have revealed β1-mediated intermolecular sheets, suggesting that the β1 strand may contribute to a possible initiation site for β-sheet-mediated PrP^{Sc} propagation. This β1 strand contains the polymorphic residue 129 that influences disease susceptibility and phenotype. To investigate the effect of the residue 129 polymorphism on the conformation of amyloid-like continuous β-sheets formed by β1, crystal structures of β1 peptides containing each of the polymorphic residues were determined. To probe the conformational influence of the peptide construct design, four different lengths of β1 peptides were studied. From the 12 peptides studied, 11 yielded crystal structures ranging in resolution from 0.9 to 1.4 Å. This ensemble of β1 crystal structures reveals conformational differences that are influenced by both the nature of the polymorphic residue and the extent of the peptide construct, indicating that comprehensive studies in which peptide constructs vary are a more rigorous approach to surveying conformational possibilities.

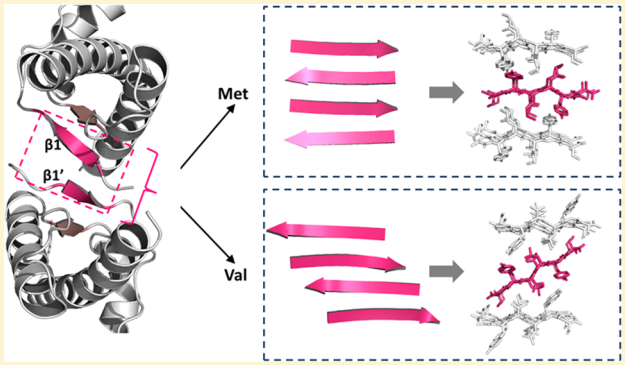

The transmissible spongiform encephalopathies (TSEs), or prion diseases, make up a group of fatal neurodegenerative disorders that affect both humans and animals.[1−3] The most common human prion disease is Creutzfeldt-Jakob disease (CJD), which can be sporadic, inherited (familial CJD), or transmitted (e.g., variant and iatrogenic CJD).[4] TSEs are unusual diseases in that the infectious prions are proteinaceous, with the conformational conversion of normal cellular prion protein (PrP^C) to the pathogenic scrapie form (PrP^{Sc}) playing a central role.[5]

To understand the mechanism of prion diseases, PrP structural studies are essential. High-resolution structures of PrP^C from various species have been determined by both crystallography and nuclear magnetic resonance (for example, refs 6−9) and show a conserved fold for the ordered C-terminal domain consisting of a small two-stranded antiparallel β-sheet (β1−β2) and three α-helices. PrP^{Sc} structural studies are complicated by the protein's insoluble, aggregated nature. Low-resolution spectroscopic studies revealed that in contrast to PrP^C, PrP^{Sc} has very little helical content and its secondary structure is primarily β-sheet.[10] The conformational conversion to PrP^{Sc} is thus understood to involve refolding of α-helical monomers to β-sheet-rich aggregates such that susceptibility to proteolysis is decreased.[11]

In the absence of high-resolution PrP^{Sc} structural information, some features of PrP^C structures suggest specific regions that may play a role in PrP^{Sc} conversion. For example, several crystal structures of human, sheep, and rabbit PrP^C show that β1 strands from adjacent monomers can interact with each other to form a continuous intermolecular antiparallel β-sheet.[12−16] This observation led to the speculation that a β1-mediated intermolecular sheet may play a role in PrP^{Sc} conversion, perhaps by acting as an initiation point.[15] Recently, crystal structures of PrP^C bound to small molecules with antiprion activity or to an inhibitory nanobody revealed that the flexible residues N-terminal to β1 fold back to H-bond to β1, thus extending the internal β-sheet to three strands[17,18] and, as a result, also preventing the formation of β1-mediated intermolecular sheets.

Also supporting the possibility that β1 may be important in the PrP^{Sc} conversion is the observation that polymorphic residue 129 that influences disease susceptibility and phenotype is located in this strand. In humans, the M/V 129 polymorphism is associated with differing susceptibilities to sporadic and transmitted CJDs, and also with distinct phenotypes of some inherited prion diseases.[19−21] In elk, the M/L polymorphism at the homologous position 132 modulates the incubation time of chronic wasting disease and influences susceptibility in a strain-dependent fashion.[22−25] PrP^Cs containing either M129 or V129 exhibit no appreciable difference in stability or protein fold.[8,14,26] Instead, several crystal structures of PrP^C disease mutants revealed that the M/V 129 polymorphism can alter the formation and conformation of β1-mediated intermolecular sheets.[14]

Received: January 26, 2015
Published: May 15, 2015

DOI: 10.1021/acs.biochem.5b00425
Biochemistry 2015, 54, 3640−3648

Table 1. Crystal Forms and Refinement Results for β1 Peptide Structures

peptide	PDB entry	resolution (Å)	R/R_{free} (%)	space group	unit cell
Group I (126−131)					
GGYMLG$_{(126-131)}$	4TUT	0.90	7.00/9.80	$P2_1$	a = 10.39 Å, b = 9.73 Å, c = 17.38 Å, β = 105.94°
GGYVLG$_{(126-131)}$	4UBY	1.00	12.01/15.77	$P1$	a = 11.67 Å, b = 17.15 Å, c = 19.07 Å, α = 79.76°, β = 86.51°, γ = 90.20°
GGYLLG$_{(126-131)}$	4UBZ	1.00	8.77/11.04	$P2_1$	a = 11.61 Å, b = 18.11 Å, c = 17.84 Å, β = 105.24°
Group II (126−132)					
GGYMLGS$_{(126-132)}$	4W5M	1.20	19.55/25.64	$C2$	a = 47.48 Å, b = 9.44 Å, c = 22.62 Å, β = 95.18°
GGYVLGS$_{(126-132)}$	4W5P	1.15	11.93/15.08	$P2_1$	a = 11.59 Å, b = 17.15 Å, c = 19.84 Å, β = 100.70°
GGYLLGS$_{(126-132)}$	4W5L	1.00	16.82/17.69	$P2_12_12$	a = 50.48 Å, b = 21.11 Å, c = 9.43 Å
Group III (127−132)					
GYMLGS$_{(127-132)}$	4WBU	1.15	15.00/16.65	$P2_12_12_1$	a = 9.44 Å, b = 17.79 Å, c = 44.56 Å
GYVLGS$_{(127-132)}$	4WBV	1.40	15.29/22.85	$P2_1$	a = 19.62 Å, b = 9.46 Å, c = 19.67 Å, β = 92.92°
Group IV (127−133)					
GYMLGSA$_{(127-133)}$	4W5Y	1.12	8.12/10.00	$P1$	a = 9.47 Å, b = 10.44 Å, c = 21.99 Å, α = 79.75°, β = 81.89°, γ = 66.75°
GYVLGSA$_{(127-133)}$	4W67	1.00	10.86/14.82	$P1$	a = 8.52 Å, b = 9.54 Å, c = 25.41 Å, α = 99.94°, β = 99.56°, γ = 90.10°
GYLLGSA$_{(127-133)}$	4W71	1.00	11.76/15.34	$P1$	a = 9.47 Å, b = 10.38 Å, c = 22.34 Å, α = 81.80°, β = 81.40°, γ = 67.95°

Because structures of aggregated proteins such as PrP^{Sc} are difficult to study at high resolution, peptides containing short segments of their corresponding native proteins have been used as models to probe amyloid structures that may resemble parts of the intact aggregated proteins.[27−34] Many of these peptides revealed amyloid-like crystal structures containing continuous β-sheets packed against each other at "steric zipper" interfaces.[27−32,34] Among peptide structures derived from a variety of amyloidogenic proteins, eight different classes of steric zipper structures corresponding to different conformations and orientations of the packed sheets have been observed.[28]

Crystal structures of several different PrP peptide segments have been reported.[28,33−35] To probe the structural consequences of the M/V/L polymorphism at position 129 and the possible effects of peptide construct design (sequence range and length) on the resulting steric zipper structure, 12 different human PrP β1 peptides were targeted for crystallization studies. The 11 resulting crystal structures show a variety of β-sheet conformations and packing geometries that are described here.

EXPERIMENTAL PROCEDURES

Peptide Design and Preparation. To increase the chances of successful crystallization and to explore possible effects of construct design, four different lengths of peptides containing PrP β1 residues were obtained. These four constructs encompass PrP residues 126−131 ("Group I"), 126−132 ("Group II"), 127−132 ("Group III"), and 127−133 ("Group IV"). For each construct, three different peptides were obtained, containing one of the polymorphic residues (methionine, valine, and leucine) at position 129. A total of 12 peptides were obtained by custom peptide synthesis (Genscript). The lyophilized peptides were dissolved in distilled water to maximal concentrations varying from 5 to 50 mg/mL and passed through a 0.22 um filter (Millipore) before being used. Remaining peptide solutions were stored at −80 °C and thawed for subsequent use.

Crystallization, Data Collection, and Structure Determination. Crystallization trials were conducted by sitting drop vapor diffusion and included exploring conditions in commercial screens as well as expanding on conditions successful for similar peptides. Details of crystallization conditions and structure determination can be found in the Supporting Information. Peptide crystals grew as either thin needles or thin plates and required data collection at microdiffraction beamlines at the Advanced Photon Source (Argonne National Laboratory, Argonne, IL). Data processing was performed using HKL2000,[36] and structure determination was conducted by direct methods with SHELXD[37] when the data resolution permitted (at 1.15 Å resolution or higher) and by molecular replacement with either Phaser[38,39] or EPMR[40] when limited by resolution. Structure refinement was performed using Phenix[41] and SHELXL,[37] and graphical model rebuilding was conducted with Coot.[42] All molecular figures were prepared using PyMol (Schrödinger). A summary of the structures is given in Table 1; detailed data collection and refinement statistics are listed in Tables S1−S4 of the Supporting Information. During the course of this work, crystal structures of two Group III peptides were reported [Protein Data Bank (PDB) entries 3NHC and 3NHD[27]]. For GYMLGS$_{(127-132)}$, the previously reported and current crystals grew from different conditions (see the Supporting Information) but have the same space group and similar unit cell dimensions and exhibit isomorphous structures. The structure reported here is refined against significantly higher resolution data (1.15 Å vs the previous 1.57 Å). For GYVLGS$_{(127-132)}$, the previously reported and current crystals not only were obtained from different conditions (see the Supporting Information) but also have different space groups and unit cell dimensions. These two GYVLGS$_{(127-132)}$ crystal forms reveal similar structural features, with the structure reported here being refined to significantly higher resolution (1.40 Å vs 1.92 Å).

Structure Analysis. There are two types of interfaces between peptides in the ensemble of PrP β1 crystal structures: the interpeptide surfaces within β-sheets and the surfaces between β-sheets. To quantitatively analyze and compare these interfaces, buried accessible surface values were calculated for both types of interfaces, and the shape complementarity was evaluated for the intersheet steric zipper interfaces, using AREAIMOL[39,43,44] and SC.[39,45−48] The surface accessibility for the polymorphic residue at position 129 was also calculated, to aid evaluation of this residue's participation in intermolecular interactions (Table S5 of the Supporting Information). Detailed explanations of these surface calculations are provided in the Supporting Information (Figures S1−S3).

DOI: 10.1021/acs.biochem.5b00425
Biochemistry 2015, 54, 3640−3648

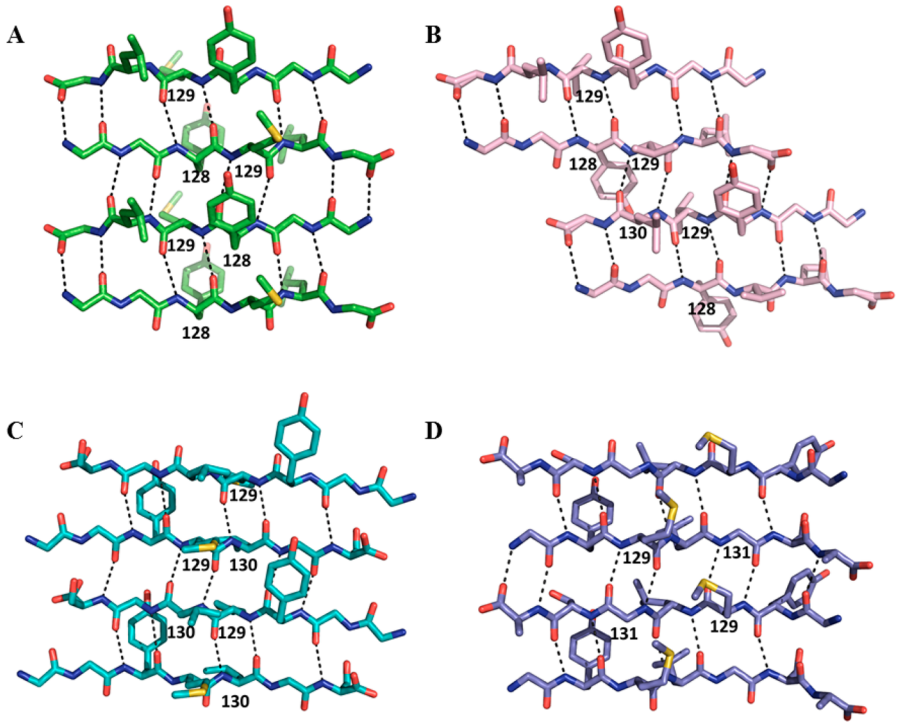

Figure 1. Representatives of the four observed types of antiparallel β-sheet H-bonding. (A) In GGYMLG$_{(126-131)}$ (green carbon atoms), each M129 forms H-bonds with Y128 in an adjacent strand. Peptides are shown as stick structures; H-bonds are drawn as dashed lines with residues 129 and their H-bond partners labeled. (B) In GGYVLG$_{(126-131)}$ (pink carbon atoms), V129 forms alternating H-bonds with Y128 and L130. (C) M129 in GGYMLGS$_{(126-132)}$ (cyan carbon atoms) forms H-bonds with L130. (D) In GYMLGSA$_{(127-133)}$ (blue carbon atoms), M129 H-bonds to G131.

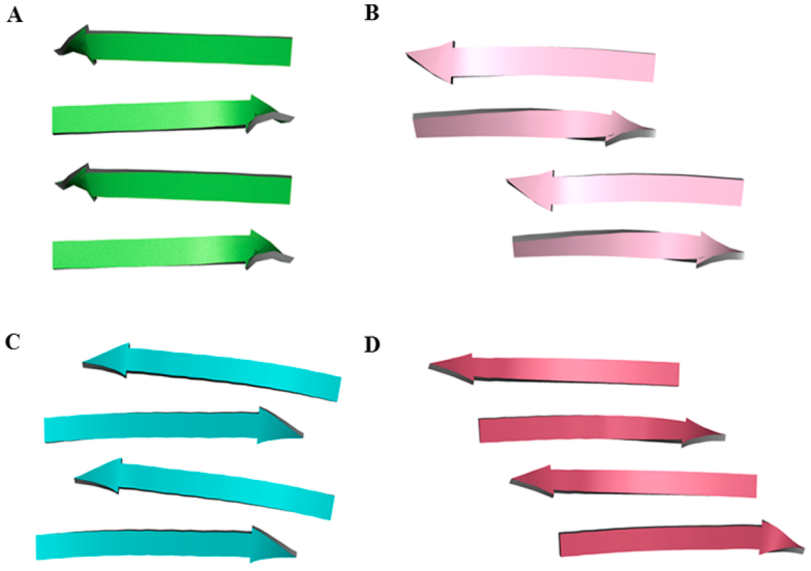

Figure 2. Examples of the four observed types of β-strand alignment. (A) In GGYMLG$_{(126-131)}$, β-strands (ribbon representation) have aligned termini. (B) In GGYVLG$_{(126-131)}$, strands are shifted in pairs. (C) In GGYMLGS$_{(126-132)}$, strands are staggered. (D) In GGYVLGS$_{(126-132)}$, strands are progressively shifted.

RESULTS

Twelve peptides containing the β1 residues that are observed to H-bond to β2 in PrP protein crystal structures were targeted for crystallization. These peptides were designed using four different β1 peptide lengths: Group I peptides with PrP residues 126−131, Group II with residues 126−132, Group III with residues 127−132, and Group IV with residues 127−133. In each group, three peptides containing either methionine, valine, or leucine at position 129, corresponding to sequence polymorphisms observed in human and elk PrPs, were studied. Diffracting crystals and subsequent refined structures were obtained for 11 of the peptides, with only the L129 variant of the 127−132 peptide failing to give useful diffraction data. While all peptides gave very thin needles or fibrils under a variety of conditions, the best diffracting crystals came from conditions unique to each peptide. Five space groups were observed among the 11 crystallized peptides, but the significant differences in the unit cell dimensions indicate that none of

DOI: 10.1021/acs.biochem.5b00425
Biochemistry 2015, 54, 3640−3648

these crystal structures are isomorphous to any other (Table 1 and Tables S1−S4 of the Supporting Information). Nine of the peptide crystal structures contain two independent peptide molecules in each asymmetric unit; the Group I peptide structures, GGYVLG$_{(126-131)}$ and GGYMLG$_{(126-131)}$, with one and four peptides in their asymmetric units, respectively, are the only exceptions. The peptide structures were refined against data to resolutions ranging from 0.9 to 1.4 Å, corresponding in most cases to atomic resolution.

PrP β1 Peptides Crystallize as Continuous Antiparallel β-Sheets Forming Steric Zippers. All 11 PrP β1 crystal structures show similar overall structures: these peptides all form continuous antiparallel β-sheets that pack against each other to form steric zippers. While the overall structures are similar, comparison of their details highlights distinct variation in the structures of the β-sheets and the geometry of their packing. Conformational variation is observed at multiple levels: in the H-bonding register within β-sheets (Figure 1), in the alignment pattern of peptide termini within the sheets (Figure 2), in the facial orientation of the β-sheets as they pack against each other to form steric zippers (Figure 3), and in the angular packing orientation of the sheets (Figure 4). A detailed comparison of these 11 peptide structures provides some insight into the influence of the M/V/L polymorphism at position 129 and of the different construct lengths on the steric zipper conformation.

Hydrogen Bonding within β1 Sheets Varies in Register. While all 11 β1 crystal structures contain antiparallel β-sheets, the alignment of H-bonds within the sheets varies (Table 2). These alignments fall into four groups that can be uniquely described by the hydrogen bonding partner(s) for the M/V/L129 residue. (a) M129 has only Y128 as its H-bonding partner [GGYMLG$_{(126-131)}$ (Figure 1A and Figure S4A of the Supporting Information)]. (b) V/L 129 forms H-bonds with Y128 and L130 in alternating strands [GGY(V/L)LG$_{(126-131)}$ and GGYVLGS$_{(126-132)}$ (Figure 1B and Figures S4B,C and S6B of the Supporting Information)]. (c) M/V/L H-bonds to only L130 [GGY(M/L)LGS$_{(126-132)}$ and GY(M/V)LGS$_{(127-132)}$ (Figure 1C and Figures S6A,C and S9A,C of the Supporting Information)]. (d) M/V/L in the three Group IV peptides forms H-bonds to only G131 [GY(M/V/L)LGSA$_{(127-133)}$ (Figure 1D and Figure S11A−C of the Supporting Information)]. The H-bonding alignment appears to be dependent on the nature of the M/V/L residue at position 129 and/or on the peptide construct in some cases, and less dependent in others. For example, the alignment with H-bonds between M/V/L129 and G131 is seen in only the Group IV (127−133) peptides, but for all three polymorphisms, so it appears to be construct-dependent. In contrast, the alternating pattern of V/L 129 H-bonding to Y128 and L130 is seen in Group I (126−131) and II (126−132) structures, but not when M129 is present, thus appearing to be as dependent on the 129 polymorphic residue as on the construct.

β1 Peptides Vary in the Alignment of Their Termini within Sheets. Just as the M/V/L129 polymorphism and peptide construct contribute to variability in the H-bonding pattern within the β1 sheets, they also give rise to differences in alignment of the peptide termini within sheets (Table 2). The 11 β1 crystal structures exhibit four different types of strand alignment: (a) all strands aligned within each sheet [GGYMLG$_{(126-131)}$, GY(M/V)LGS$_{(127-132)}$, and GY(M/V/L)LGSA$_{(127-133)}$ (Figure 2A and Figures S4A, S9A,C, and S11A−C of the Supporting Information)], (b) strands that shift in pairs [GGY(V/L)LG$_{(126-131)}$ (Figure 2B and Figure S4B,C of the Supporting Information)], (c) strands that are staggered, alternating in the alignment of their termini [GGY(M/L)LGS$_{(126-132)}$ (Figure 2C and Figure S6A,C of the Supporting Information)], and (d) strands the shift continuously [GGYVLGS$_{(126-132)}$ (Figure 2D and Figure S6B of the Supporting Information)]. The β1 strand alignment appears to be dependent on the peptide construct; for example, all Group III and IV structures contain sheets with well-aligned strands. However, the M/V/L residue at position 129 also appears to influence the strand alignment in other constructs. Group I structures containing V/L 129 have strands shifted in pairs, but that containing M129 has aligned strands. Group II structures with M/L 129 have staggered strands, while that containing V129 has continuously shifted strands. Strand

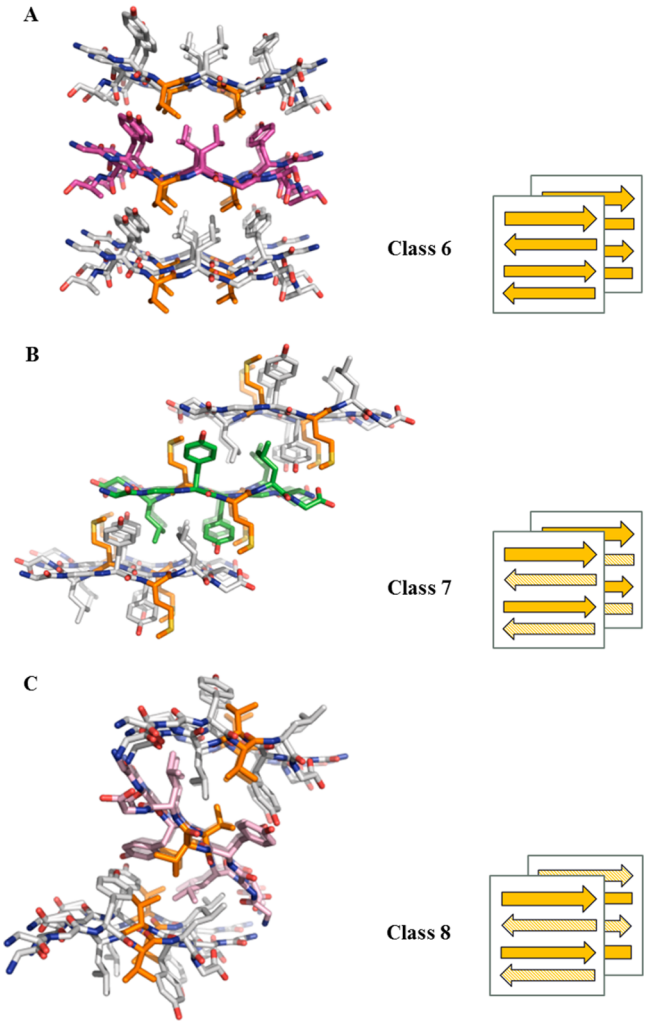

Figure 3. Representatives of the three observed types of steric zippers. (A) GYVLGSA$_{(127-133)}$ forms a Class 6 steric zipper. Three layers of β-sheets are shown, with the middle sheet colored (magenta carbon atoms). Four strands of each continuous β-sheet are shown, with the side chain of M129 highlighted with orange carbon atoms. (B) GGYMLG$_{(126-131)}$ (middle sheet with green carbon atoms) forms a Class 7 steric zipper. C) GGYVLG$_{(126-131)}$ (middle sheet with pink carbon atoms) forms a Class 8 steric zipper. The diagram accompanying each structure shows the orientation of strands in adjacent sheets in simplified fashion, with the opposite faces of each strand colored different shades of yellow.

DOI: 10.1021/acs.biochem.5b00425
Biochemistry 2015, 54, 3640−3648

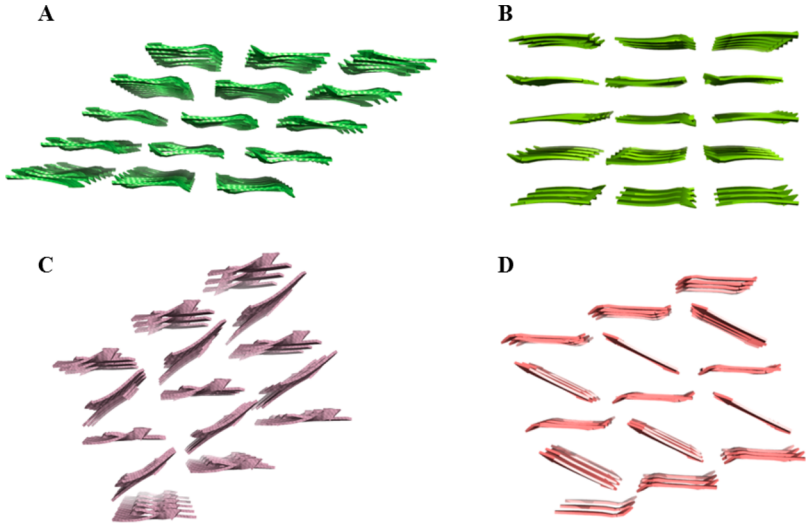

Figure 4. Examples of the different observed types of sheet packing. (A) $GGYMLG_{(126-131)}$ β-sheets are packed flat against each other and shifted. (B) $GYMLGS_{(127-132)}$ sheets pack flat and are aligned. (C) $GGYVLG_{(126-131)}$ sheets are tilted in alternating layers to give open triangles. (D) $GYVLGS_{(127-132)}$ sheets are also tilted in alternating layers, but with termini aligned to form closed parallelograms.

Table 2. Summary of Observations for β1 Peptide Structures

peptide	strand alignment	residue 129 H-bond partner(s)	steric zipper class	sheet packing type
Group I (126−131)				
$GGYMLG_{(126-131)}$	aligned	128	7	flat, shifted
$GGYVLG_{(126-131)}$	pairwise shift	128, 130	8	tilted, open (1)
$GGYLLG_{(126-131)}$	pairwise shift	128, 130	8	tilted, open (2)
Group II (126−132)				
$GGYMLGS_{(126-132)}$	staggered	130	8	tilted, closed
$GGYVLGS_{(126-132)}$	continuous shift	128, 130	8	tilted, open
$GGYLLGS_{(126-132)}$	staggered	130	8	tilted, closed
Group III (127−132)				
$GYMLGS_{(127-132)}$	aligned	130	8	flat, aligned
GYMLGS[a] (3NHC)	aligned	130	8	flat, aligned
$GYVLGS_{(127-132)}$	aligned	130	8	tilted, closed
GYVLGS[a] (3NHD)	aligned	130	8	tilted, closed
Group IV (127−133)				
$GYMLGSA_{(127-133)}$	aligned	131	6	flat, shifted
$GYVLGSA_{(127-133)}$	aligned	131	6	flat, aligned
$GYLLGSA_{(127-133)}$	aligned	131	6	flat, shifted

[a]3NHC and 3NHD were previously reported.[27]

alignment correlates with H-bond register within peptide construct groups, as expected, but not across groups (Table 2).

β1 Sheets Form Steric Zippers That Fall into Different Classes. The β1 antiparallel sheets pack against each other with their side chains intercalating and forming steric zipper interfaces. Previous studies have shown that steric zipper structures can be classified according to the facial and directional alignment of the interacting β-sheets.[28] The 11 PrP β1 crystal structures can be grouped into three steric zipper classes (Table 2). All of the Group IV peptides form Class 6 steric zippers, with all the strands within each sheet facing the same direction, and adjacent sheets forming the steric zipper also facing the same direction [$GY(M/V/L)LGSA_{(127-133)}$ (Figure 3A and Figure S12A−C of the Supporting Information)]. These represent the first observation of Class 6 steric zippers formed by PrP β1 peptides. Only the $GGYMLG_{(126-131)}$ structure forms a Class 7 steric zipper, with the strands within each sheet alternating in their facial orientation but with adjacent sheets forming the steric zipper all facing the same direction (Figure 3B and Figure S5A of the Supporting Information). The seven remaining structures, two of the three Group I peptides and all Group II and III peptides, have Class 8 steric zippers, with the strands within each sheet alternating in their facial orientation and aligned strands in adjacent sheets also alternating in their facial orientation [$GGY(V/L)LG_{(126-131)}$, $GGY(M/V/L)LGS_{(126-132)}$, and $GY(M/V)LGS_{(127-132)}$ (Figure 3C and Figure S5B,C, S7A−C, and S10A,0C of the Supporting Information). The Group II−IV peptides form the same steric zippers within each group, indicating that the M/V/L129 polymorphism does not alter the geometry of the steric zippers formed. It is only within the Group I structures that more than one type of steric zipper class is observed.

β1 Steric Zippers Pack with Varying Orientations and Alignments. The 11 β1 peptide structures fall into three different steric zipper classes. Additional striking differences are also observed in the orientation of the sheets forming the steric zippers, which can be flat or tilted, and how the ends of the sheets are aligned with each other (Table 2). In five structures, the steric zippers are formed by adjacent sheets packing flat against each other, either with shifted ends [$GGYMLG_{(126-131)}$ and $GY(M/L)LGSA_{(127-133)}$ (Figure 4A and Figures S5A and S12A,C of the Supporting Information)] or with ends aligned [$GYMLGS_{(127-132)}$ and $GYVLGSA_{(127-133)}$ (Figure 4B and Figures S10A and S12B of the Supporting Information)]. In the other six structures, the steric zippers form such that alternating layers of sheets are tilted with respect to each other [GGY(V/

DOI: 10.1021/acs.biochem.5b00425
Biochemistry 2015, 54, 3640−3648

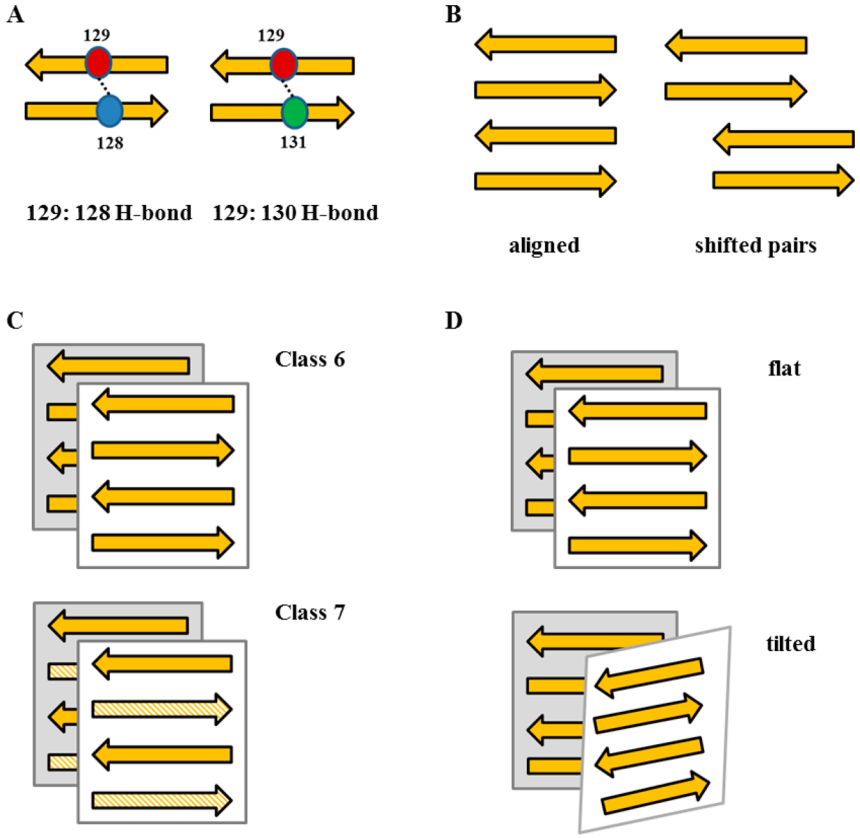

Figure 5. β1 peptide structures exhibit conformational variability on multiple levels. The ensemble of PrP β1 peptide crystal structures reveals variability in (A) β-sheet H-bonding register, (B) alignment of β-strand termini within each sheet, (C) the orientation of packing between sheets, and (D) the angle of packing within sheets. Two representative examples are given for each of these four conformational characteristics to illustrate the observed variability.

L)LG$_{(126-131)}$, GGY(M/V/L)LGS$_{(126-132)}$, and GYVLGS$_{(127-132)}$ (Figure 4C,D and Figures S5B,C, S7A–C, and S10C of the Supporting Information)].

Within the group of tilted steric zippers, there are subtle differences in the sheet alignments that become apparent when they are viewed from the side of the sheets. For example, in the GGYVLG$_{(126-131)}$ structure, the layers of sheets are arranged to form "open" triangles (Figure 4C and Figure S5B of the Supporting Information), while in the GYVLGS$_{(127-132)}$ structure, the alternating layers of sheets are arranged such that they form "closed" parallelograms (Figure 4D and Figure S10C of the Supporting Information). Even among the "open" tilted steric zippers, different orientations are observed, such as for GGYVLG$_{(126-131)}$ and GGYLLG$_{(126-131)}$ (Figure S5B,C and Table 2). The flat versus tilted orientation of steric zippers formed by β1 sheets appears to be influenced by both the peptide construct and the M/V/L129 polymorphism. For example, all Group II structures have tilted steric zippers, while all Group IV structures have flat steric zippers, reflecting the influence of the peptide construct. However, within the Group II structures, both "open" and "closed" tilted arrangements are observed; similarly, within the Group IV structures, both shifted and aligned flat steric zippers are observed, reflecting the influence of the M/V/L129 polymorphism.

DISCUSSION

The 11 PrP β1 peptides in this study all crystallize to form continuous β-sheets that pack together with intercalating side chains at steric zipper interfaces. The two Group III peptides were previously crystallized under conditions different from those reported here[27] (Supporting Information). The GYMLGS$_{(127-132)}$ crystals described here and reported earlier are isomorphous, with the major differences being improved resolution (1.15 Å here vs 1.57 Å earlier) and five additional water molecules included in the final refined structure. In contrast, the crystals reported here and earlier for GYVLGS$_{(127-132)}$ have nonisomorphous space groups and unit cells; differences include improved resolution (1.15 Å here vs 1.57 Å earlier), numbers of peptides in each asymmetric unit (two here vs one earlier), and the number and identity of solvent molecules included in the refined structures (Supporting Information). It is important to note that similar peptide and β-zipper conformations were observed for the two isomorphous GYMLGS$_{(127-132)}$ crystals, and also for the two nonisomorphous GYVLGS$_{(127-132)}$ crystals. For these two sets of structures, different crystallization conditions and crystal forms did not alter the H-bond or strand alignment within the β-sheets or the orientation of the stacking of the sheets against each other (Table 2 and Figures S8–S10 of the Supporting Information). This observation suggests that the structural differences among β1 peptide structures are driven by differences between the peptide sequences and construct design and are not crystallization artifacts.

A detailed comparison of the 11 β1 crystal structures reveals a diversity of conformations that can be distinguished at four different levels (Table 2 and Figure 5). First, four different types of H-bonding alignment between strands within the sheets are observed. Four different types of strand termini

DOI: 10.1021/acs.biochem.5b00425
Biochemistry 2015, 54, 3640–3648

alignment are also observed; these do not correlate exactly with the different types of H-bonding alignment. Three different classes of steric zipper interfaces are observed, each representing a different combination of facial and directional alignment of the strands in the interacting sheets. Finally, the continuous β-sheets are observed to pack either flat against each other or in a tilted fashion, with variations within each of these two types of interactions. Altogether, the 11 β1 crystals reveal nine distinct steric zipper conformations, resulting from distinct combinations of different types of intra- and intersheet interactions.

Peptide Construct Extent Influences the β1 Steric Zipper Structure. The design of the β1 peptide construct, i.e., the extent of the PrP sequence included in the peptide design, appears to have a strong but not completely defining influence on the observed β-sheet and steric zipper conformations (Table 2). For example, peptides within Group IV (residues 127−133) all exhibit the same H-bond register, alignment of strand termini, and steric zipper class, regardless of the M/V/L129 polymorphic residue present. The two Group III peptides (residues 127−132) also share the same conformational features as described at these three levels. The peptide construct appears to be still influential but a less determining factor for the Group I and II peptides (126−131 and 126−132, respectively); in each of these two groups, two types of combinations of H-bond register, strand alignment, and steric zipper class are observed. It is interesting to note that while the same steric zipper conformation may be observed in more than one peptide within a construct group, there is no similar steric zipper conformation that is observed in peptides belonging to two different construct groups, reflecting the strong influence of the peptide residue range on the observed steric zipper structure.

The M/V/L129 Polymorphic Residue Is Associated with Structural Variation. Within each of the four peptide construct groups, peptides each containing a different M/V/L polymorphic residue at position 129 were studied, and the sequence variation resulted in conformational differences (Table 2). For example, the Group IV peptides have similar H-bond register, strand alignment, and steric zipper class; however, the V129 sheets pack flat and aligned, while the M/L 129 sheets pack flat and shifted. Similarly, in Group III, the V129 structure differs from the M129 structure only in the orientation of the steric zipper packing ("closed" tilted vs flat and aligned). The contribution of the M/V/L129 polymorphism appears to be more significant in the Group I and II peptide structures. For the Group I peptides, the M129 structure differs in H-bond register, strand alignment, and steric zipper class from the V/L 129 structures; the three peptides give rise to three different orientations of steric zipper packing. In the Group II structures, V129 has a unique conformation while the M/L 129 structures are very similar to each other.

Within each of the four peptide construct groups, there is always a conformational difference between the M129 and V129 structures, although the nature of the difference is unique to each construct group. In Group I, the M/V 129 polymorphism alters H-bond register, strand alignment, steric zipper class, and steric zipper packing orientation. In Group II, the steric zipper class is the same for the M/V 129 structures but the other three levels of conformation differ. Within Groups III and IV, the M/V 129 structures are similar except for the orientation of the steric zipper packing. Taken together, the peptide structures show that the M/V 129 polymorphism does alter steric zipper conformation, regardless of peptide construct design. The influence of the M/L 129 polymorphism on peptide conformation is less consistent. In the Group II and IV peptides, the L129 structure is very similar to the M129 structure, and different from the corresponding V129 structure. In Group I, all three M/V/L129 structures are different from each other.

In an attempt to quantify the conformational differences among the β1 peptides, for each structure values were calculated for: the accessible surface buried between adjacent strands within the same sheet, the buried accessible surface and shape complementarity of strands in adjacent sheets forming the steric zipper interface, and the loss of accessible surface area for the 129 residue in the steric zipper structure, compared to its exposure in an isolated peptide (Table S5 of the Supporting Information). For peptides in Groups I, III, and IV, the degree to which the polymorphic residue 129's surface is buried upon formation of the steric zipper correlates best with the observed conformational differences. For example, in Group I, three different steric zipper conformations are observed for the M/V/L129 structures, for which three different values for the relative accessible surface area reduction for residue 129 can be calculated. In Group IV, the M/L 129 steric zippers are similar to each other and different from V129; this pattern is also seen for their respective values calculated for the relative reduction in accessible surface area for residue 129. For Group II peptides, the accessible surface area buried between strands within each sheet better correlates with the steric zipper differences among the three structures, likely due to the differences in H-bond register and strand alignment within the sheets.

CONCLUSION

The 11 PrP β1 crystal structures described here sample four different peptide constructs as well as the different M/V/L129 polymorphic residues. They give rise to nine distinct steric zipper conformations that appear to be influenced strongly by both the residue extent of the peptide construct as well as the nature of the polymorphic residue. Comparison with two previously reported Group III peptide structures indicates that peptide and steric zipper conformations are driven by differences between the peptide sequences and construct design and are not crystallization artifacts.

The M/V 129 polymorphism is associated with human prion disease susceptibility and phenotype. Within each of the four construct groups, the M129 and V129 structures show differences in steric zipper conformations, although the conformations for each polymorphism differ also between the different constructs. The conformational differences correlate with the many reports of the M/V129 polymorphism being associated with susceptibility to infectious prion diseases such as the bovine spongiform encephalopathy-related variant CJD and kuru,[21,49] the phenotype of inherited prion diseases,[20] and also susceptibility to sporadic disease forms of unknown origin.[19]

In contrast, the protective effects of the M/L132 elk polymorphism (corresponding to residue 129 in hPrP) in chronic wasting disease (CWD) are highly strain dependent.[22−25] Biophysical and infectivity studies indicate that often different prion disease strains correspond to different conformational strains.[50−53] In the work presented here, the L129 peptide structure is different from both M129 and V129 peptides in Group I, and similar to the M129 peptide in Groups II and IV. Thus, the M/L129 steric zipper conformational

DOI: 10.1021/acs.biochem.5b00425
Biochemistry 2015, 54, 3640−3648

similarity or difference is construct-dependent, which may reflect the strain dependence of the M/L129 protective effect.

Because the steric zipper conformations for any particular M/V/L129 polymorphism are different across the four peptide construct groups, it is unclear whether any specific conformation observed in this ensemble of structures is relevant to the prion disease mechanism. Alternatively, because many prion disease strains have been characterized, and many of those have been attributed to different conformational strains,[50−53] it is possible that the different steric zipper conformations observed here reflect the conformational diversity among prion disease strains and/or variations in disease mechanism for different strains. The conformational differences are observed between M129 and V129 structures across the four peptide construct groups, which reflects the consistency of the association of M/V129 polymorphism with disease propensity and phenotype for a variety of infectious, inherited, and sporadic human prion diseases. In contrast, the conformational difference between M129 and L129 peptide structures is less consistently observed and appears to be highly dependent on peptide construct design, perhaps reflecting the observation that the protective effect of the L129 polymorphism in chronic wasting disease is strain-dependent.

The correlation between the pattern of peptide structural differences and the degree of association of polymorphism with disease propensity, phenotype, and strain dependence suggests that peptide studies remain informative models for amyloid proteins such as PrP^{Sc}.[27−34] These studies suggest that varying peptide construct design as an additional experimental parameter provides for a more complete survey of conformational possibilities. However, the diversity of conformations observed across peptide construct groups warns against overinterpretation of specific steric zipper conformations, whose mechanistic relevance awaits future studies.

■ ASSOCIATED CONTENT

Supporting Information

Supplemental methods, tables, and figures. The Supporting Information is available free of charge on the ACS Publications website at DOI: 10.1021/acs.biochem.5b00425.

■ AUTHOR INFORMATION

Corresponding Author

*E-mail: vivien.yee@case.edu. Telephone: (216) 368-1184.

Present Address

†S.-J.L.: Warp Drive Bio, LLC, Cambridge, MA 02139.

Funding

This work was partially supported by a Brain Disorders Award from the McKnight Endowment Fund for Neurosciences and National Institutes of Health Grant DK075897 to V.C.Y.

Notes

The authors declare no competing financial interest.

■ ACKNOWLEDGMENTS

We thank Dr. Witold Surewicz for helpful discussions. Diffraction data were measured at the Structural Biology Center and GM/CA beamlines at the Advanced Photon Source. GM/CA @ APS has been funded in whole or in part with federal funds from the National Cancer Institute (Y1-CO-1020) and the National Institute of General Medical Sciences (Y1-GM-1104). Use of the Advanced Photon Source was supported by the U.S. Department of Energy, Basic Energy Sciences, Office of Science, under Contract DE-AC02-06CH11357. Coordinate and structure factor files have been deposited in the Protein Data Bank (entries listed in Table 1).

■ ABBREVIATIONS

PrP, prion protein; PrP^{C}, cellular prion protein; PrP^{Sc}, scrapie prion protein; $GGY\underline{M}LG_{(126-131)}$, peptide containing PrP residues 126−131, with the polymorphic residue at position 129 underlined; $GY(\underline{M}/\underline{V}/\underline{L})LGSA_{(127-133)}$, peptides containing PrP residues 127−133 and either M, V, or L in polymorphic position 129.

■ REFERENCES

(1) Prusiner, S. B. (1998) Prions. *Proc. Natl. Acad. Sci. U.S.A. 95*, 13363−13383.

(2) Collinge, J. (2001) Prion diseases of humans and animals: Their causes and molecular basis. *Annu. Rev. Neurosci. 24*, 519−550.

(3) Aguzzi, A., Baumann, F., and Bremer, J. (2008) The prion's elusive reason for being. *Annu. Rev. Neurosci. 31*, 439−477.

(4) Knight, R. (2006) Creutzfeldt-Jakob disease: A rare cause of dementia in elderly persons. *Clin. Infect. Dis. 43*, 340−346.

(5) Pan, K. M., Baldwin, M., Nguyen, J., Gasset, M., Serban, A., Groth, D., Mehlhorn, I., Huang, Z., Fletterick, R. J., Cohen, F. E., et al. (1993) Conversion of α-helices into β-sheets features in the formation of the scrapie prion proteins. *Proc. Natl. Acad. Sci. U.S.A. 90*, 10962−10966.

(6) Riek, R., Hornemann, S., Wider, G., Billeter, M., Glockshuber, R., and Wuthrich, K. (1996) NMR structure of the mouse prion protein domain PrP(121−231). *Nature 382*, 180−182.

(7) James, T. L., Liu, H., Ulyanov, N. B., Farr-Jones, S., Zhang, H., Donne, D. G., Kaneko, K., Groth, D., Mehlhorn, I., Prusiner, S. B., and Cohen, F. E. (1997) Solution structure of a 142-residue recombinant prion protein corresponding to the infectious fragment of the scrapie isoform. *Proc. Natl. Acad. Sci. U.S.A. 94*, 10086−10091.

(8) Zahn, R., Liu, A., Luhrs, T., Riek, R., von Schroetter, C., Lopez Garcia, F., Billeter, M., Calzolai, L., Wider, G., and Wuthrich, K. (2000) NMR solution structure of the human prion protein. *Proc. Natl. Acad. Sci. U.S.A. 97*, 145−150.

(9) Knaus, K. J., Morillas, M., Swietnicki, W., Malone, M., Surewicz, W. K., and Yee, V. C. (2001) Crystal structure of the human prion protein reveals a mechanism for oligomerization. *Nat. Struct. Biol. 8*, 770−774.

(10) Caughey, B. W., Dong, A., Bhat, K. S., Ernst, D., Hayes, S. F., and Caughey, W. S. (1991) Secondary Structure-Analysis of the Scrapie-Associated Protein Prp 27−30 in Water by Infrared-Spectroscopy. *Biochemistry 30*, 7672−7680.

(11) Surewicz, W. K., and Apostol, M. I. (2011) Prion protein and its conformational conversion: A structural perspective. *Top. Curr. Chem. 305*, 135−167.

(12) Sweeting, B., Brown, E., Khan, M. Q., Chakrabartty, A., and Pai, E. F. (2013) N-Terminal Helix-Cap in α-Helix 2 Modulates β-State Misfolding in Rabbit and Hamster Prion Proteins. *PLoS One 8*, e63047.

(13) Khan, M. Q., Sweeting, B., Mulligan, V. K., Arslan, P. E., Cashman, N. R., Pai, E. F., and Chakrabartty, A. (2010) Prion disease susceptibility is affected by β-structure folding propensity and local side-chain interactions in PrP. *Proc. Natl. Acad. Sci. U.S.A. 107*, 19808−19813.

(14) Lee, S., Antony, L., Hartmann, R., Knaus, K. J., Surewicz, K., Surewicz, W. K., and Yee, V. C. (2010) Conformational diversity in prion protein variants influences intermolecular β-sheet formation. *EMBO J. 29*, 251−262.

(15) Haire, L. F., Whyte, S. M., Vasisht, N., Gill, A. C., Verma, C., Dodson, E. J., Dodson, G. G., and Bayley, P. M. (2004) The crystal structure of the globular domain of sheep prion protein. *J. Mol. Biol. 336*, 1175−1183.

DOI: 10.1021/acs.biochem.5b00425
Biochemistry 2015, 54, 3640−3648

(16) Antonyuk, S. V., Trevitt, C. R., Strange, R. W., Jackson, G. S., Sangar, D., Batchelor, M., Cooper, S., Fraser, C., Jones, S., Georgiou, T., Khalili-Shirazi, A., Clarke, A. R., Hasnain, S. S., and Collinge, J. (2009) Crystal structure of human prion protein bound to a therapeutic antibody. *Proc. Natl. Acad. Sci. U.S.A. 106*, 2554−2558.
(17) Baral, P. K., Swayampakula, M., Rout, M. K., Kav, N. N., Spyracopoulos, L., Aguzzi, A., and James, M. N. (2014) Structural basis of prion inhibition by phenothiazine compounds. *Structure 22*, 291−303.
(18) Abskharon, R. N., Giachin, G., Wohlkonig, A., Soror, S. H., Pardon, E., Legname, G., and Steyaert, J. (2014) Probing the N-terminal β-sheet conversion in the crystal structure of the human prion protein bound to a nanobody. *J. Am. Chem. Soc. 136*, 937−944.
(19) Palmer, M. S., Dryden, A. J., Hughes, J. T., and Collinge, J. (1991) Homozygous prion protein genotype predisposes to sporadic Creutzfeldt-Jakob disease. *Nature 352*, 340−342.
(20) Goldfarb, L. G., Petersen, R. B., Tabaton, M., Brown, P., LeBlanc, A. C., Montagna, P., Cortelli, P., Julien, J., Vital, C., Pendelbury, W. W., et al. (1992) Fatal familial insomnia and familial Creutzfeldt-Jakob disease: Disease phenotype determined by a DNA polymorphism. *Science 258*, 806−808.
(21) Mead, S., Stumpf, M. P., Whitfield, J., Beck, J. A., Poulter, M., Campbell, T., Uphill, J. B., Goldstein, D., Alpers, M., Fisher, E. M., and Collinge, J. (2003) Balancing selection at the prion protein gene consistent with prehistoric kurulike epidemics. *Science 300*, 640−643.
(22) Green, K. M., Browning, S. R., Seward, T. S., Jewell, J. E., Ross, D. L., Green, M. A., Williams, E. S., Hoover, E. A., and Telling, G. C. (2008) The elk PRNP codon 132 polymorphism controls cervid and scrapie prion propagation. *J. Gen. Virol. 89*, 598−608.
(23) Peletto, S., Perucchini, M., Acin, C., Dalgleish, M. P., Reid, H. W., Rasero, R., Sacchi, P., Stewart, P., Caramelli, M., Ferroglio, E., Bozzetta, E., Meloni, D., Orusa, R., Robetto, S., Gennero, S., Goldmann, W., and Acutis, P. L. (2009) Genetic variability of the prion protein gene (PRNP) in wild ruminants from Italy and Scotland. *J. Vet. Sci. 10*, 115−120.
(24) Hamir, A. N., Gidlewski, T., Spraker, T. R., Miller, J. M., Creekmore, L., Crocheck, M., Cline, T., and O'Rourke, K. I. (2006) Preliminary observations of genetic susceptibility of elk (*Cervus elaphus nelsoni*) to chronic wasting disease by experimental oral inoculation. *J. Vet. Diagn. Invest. 18*, 110−114.
(25) Perucchini, M., Griffin, K., Miller, M. W., and Goldmann, W. (2008) PrP genotypes of free-ranging wapiti (*Cervus elaphus nelsoni*) with chronic wasting disease. *J. Gen. Virol. 89*, 1324−1328.
(26) Hosszu, L. L., Jackson, G. S., Trevitt, C. R., Jones, S., Batchelor, M., Bhelt, D., Prodromidou, K., Clarke, A. R., Waltho, J. P., and Collinge, J. (2004) The residue 129 polymorphism in human prion protein does not confer susceptibility to Creutzfeldt-Jakob disease by altering the structure or global stability of PrPC. *J. Biol. Chem. 279*, 28515−28521.
(27) Apostol, M. I., Sawaya, M. R., Cascio, D., and Eisenberg, D. (2010) Crystallographic Studies of Prion Protein (PrP) Segments Suggest How Structural Changes Encoded by Polymorphism at Residue 129 Modulate Susceptibility to Human Prion Disease. *J. Biol. Chem. 285*, 29671−29675.
(28) Sawaya, M. R., Sambashivan, S., Nelson, R., Ivanova, M. I., Sievers, S. A., Apostol, M. I., Thompson, M. J., Balbirnie, M., Wiltzius, J. J., McFarlane, H. T., Madsen, A. O., Riekel, C., and Eisenberg, D. (2007) Atomic structures of amyloid cross-β spines reveal varied steric zippers. *Nature 447*, 453−457.
(29) Wiltzius, J. J., Landau, M., Nelson, R., Sawaya, M. R., Apostol, M. I., Goldschmidt, L., Soriaga, A. B., Cascio, D., Rajashankar, K., and Eisenberg, D. (2009) Molecular mechanisms for protein-encoded inheritance. *Nat. Struct. Mol. Biol. 16*, 973−978.
(30) Nelson, R., Sawaya, M. R., Balbirnie, M., Madsen, A. O., Riekel, C., Grothe, R., and Eisenberg, D. (2005) Structure of the cross-β spine of amyloid-like fibrils. *Nature 435*, 773−778.
(31) Wiltzius, J. J., Sievers, S. A., Sawaya, M. R., Cascio, D., Popov, D., Riekel, C., and Eisenberg, D. (2008) Atomic structure of the cross-β spine of islet amyloid polypeptide (amylin). *Protein Sci. 17*, 1467−1474.
(32) Colletier, J. P., Laganowsky, A., Landau, M., Zhao, M., Soriaga, A. B., Goldschmidt, L., Flot, D., Cascio, D., Sawaya, M. R., and Eisenberg, D. (2011) Molecular basis for amyloid-β polymorphism. *Proc. Natl. Acad. Sci. U.S.A. 108*, 16938−16943.
(33) Apostol, M. I., Perry, K., and Surewicz, W. K. (2013) Crystal structure of a human prion protein fragment reveals a motif for oligomer formation. *J. Am. Chem. Soc. 135*, 10202−10205.
(34) Apostol, M. I., Wiltzius, J. J. W., Sawaya, M. R., Cascio, D., and Eisenberg, D. (2011) Atomic Structures Suggest Determinants of Transmission Barriers in Mammalian Prion Disease. *Biochemistry 50*, 2456−2463.
(35) Yau, J., and Sharpe, S. (2012) Structures of amyloid fibrils formed by the prion protein derived peptides PrP(244−249) and PrP(245−250). *J. Struct. Biol. 180*, 290−302.
(36) Otwinowski, Z., and Minor, W. (1997) Processing of X-ray diffraction data collected in oscillation mode. *Methods Enzymol. 276*, 307−326.
(37) Sheldrick, G. M. (2008) A short history of SHELX. *Acta Crystallogr. A64*, 112−122.
(38) McCoy, A. J., Grosse-Kunstleve, R. W., Adams, P. D., Winn, M. D., Storoni, L. C., and Read, R. J. (2007) Phaser crystallographic software. *J. Appl. Crystallogr. 40*, 658−674.
(39) Winn, M. D., Ballard, C. C., Cowtan, K. D., Dodson, E. J., Emsley, P., Evans, P. R., Keegan, R. M., Krissinel, E. B., Leslie, A. G., McCoy, A., McNicholas, S. J., Murshudov, G. N., Pannu, N. S., Potterton, E. A., Powell, H. R., Read, R. J., Vagin, A., and Wilson, K. S. (2011) Overview of the CCP4 suite and current developments. *Acta Crystallogr. D67*, 235−242.
(40) Kissinger, C. R., Gehlhaar, D. K., and Fogel, D. B. (1999) Rapid automated molecular replacement by evolutionary search. *Acta Crystallogr. D55*, 484−491.
(41) Adams, P. D., Afonine, P. V., Bunkoczi, G., Chen, V. B., Davis, I. W., Echols, N., Headd, J. J., Hung, L. W., Kapral, G. J., Grosse-Kunstleve, R. W., McCoy, A. J., Moriarty, N. W., Oeffner, R., Read, R. J., Richardson, D. C., Richardson, J. S., Terwilliger, T. C., and Zwart, P. H. (2010) PHENIX: A comprehensive Python-based system for macromolecular structure solution. *Acta Crystallogr. D66*, 213−221.
(42) Emsley, P., and Cowtan, K. (2004) Coot: Model-building tools for molecular graphics. *Acta Crystallogr. D60*, 2126−2132.
(43) Lee, B., and Richards, F. M. (1971) The interpretation of protein structures: Estimation of static accessibility. *J. Mol. Biol. 55*, 379−400.
(44) Saff, E. B., and Kuijlaars, A. B. J. (1997) Distributing many points on a sphere. *The Mathematical Intelligencer 19*, 5−11.
(45) Lawrence, M. C., and Colman, P. M. (1993) Shape Complementarity at Protein-Protein Interfaces. *J. Mol. Biol. 234*, 946−950.
(46) Richards, F. M. (1977) Areas, Volumes, Packing, and Protein-Structure. *Annu. Rev. Biophys. Bioeng. 6*, 151−176.
(47) Connolly, M. L. (1983) Analytical Molecular-Surface Calculation. *J. Appl. Crystallogr. 16*, 548−558.
(48) Nicholls, A., Bharadwaj, R., and Honig, B. (1993) Grasp: Graphical Representation and Analysis of Surface-Properties. *Biophys. J. 64*, A166.
(49) Zeidler, M., Stewart, G., Cousens, S. N., Estibeiro, K., and Will, R. G. (1997) Codon 129 genotype and new variant CJD. *Lancet 350*, 668.
(50) Collinge, J., and Clarke, A. R. (2007) A general model of prion strains and their pathogenicity. *Science 318*, 930−936.
(51) Haik, S., and Brandel, J. P. (2011) Biochemical and strain properties of CJD prions: Complexity versus simplicity. *J. Neurochem. 119*, 251−261.
(52) Weissmann, C., Li, J. L., Mahal, S. P., and Browning, S. (2011) Prions on the move. *EMBO Rep. 12*, 1109−1117.
(53) Telling, G. C. (2011) Transgenic mouse models and prion strains. *Top. Curr. Chem. 305*, 79−99.

DOI: 10.1021/acs.biochem.5b00425
Biochemistry 2015, 54, 3640−3648